High power 739 nm VECSELs for future Yb^+ ion cooling

JONATHAN R. C. WOODS,[1,*] HERMANN KAHLE,[2] ALAN C. GRAY,[3] JAKE DAYKIN,[1] ANNE C. TROPPER,[1] CORIN GAWITH,[3] MIRCEA GUINA,[2] AND VASILIS APOSTOLOPOULOS[1]

[1]*School of Physics and Astronomy, University of Southampton, University Road, Southampton, Hampshire, SO17 1BJ.*
[2]*Optoelectronics Research Centre (ORC), Physics Unit / Photonics, Faculty of Engineering and Natural Science, Tampere University, Korkeakoulunkatu 3, 33720 Tampere, Finland*
[3]*Optoelectronics Research Centre, University of Southampton, University Road, Southampton, Hampshire, SO17 1BJ.*
[*]*J.Woods@soton.ac.uk*

Abstract: We present an operational characterisation of a vertical-external-cavity surface-emitting laser (VECSEL) emitting around 739 nm with over 150 mW in a single fundamental spatial mode. Results show that the laser is capable of oscillating on a single cavity axial mode at 740 nm for up to 22 mW. Tuning of the optical emission is shown to reach 737.3 nm. Furthermore at best performance, the laser exhibits a slope efficiency of 8.3 %, and a threshold power of 1.27 W for an output coupler reflectivity of 98 %.

The spectral region between 700 and 800 nm is rich with scientific applications for laser sources that can exhibit high power, narrow linewidth, wavelength selectivity and compact dimensions. In the context of laser cooling and trapping of atoms and ions alone, direct emission in this wavelength region could be applied to species such as K [1], Rb [2] and F [3]. Equally, generating higher order harmonics of this wavelength region would permit their application for Ag [4], Ca^+ [5], Yb [6], and Yb^+ [7]. VECSELs are ideal sources for fulfilling the above requirements: they can be flexible and wavelength selective, since their emission can be tailored through careful choice of semiconductor quantum well composition and dimensions, and they typically exhibit very near diffraction limited beam profiles. VECSELs can therefore provide similar performance to conventional solid state laser sources while being significantly more compact and with less stringent pump laser requirements which, additionally, improves cost effectiveness.

Recently, Gray *et al.* [8] published a first demonstration of a periodically-poled lithium niobate (PPLN) waveguide pumped by a VECSEL emitting natively around 780 nm, where 1 mW of 390 nm light was generated via second harmonic generation (SHG). This article presents a proof of principle system for generation of UV light and show cases a VECSEL as future competition to the well established Ti:Sapphire laser source; VECSELs can be made with very small external cavities while still providing spectrally pure, watt level emission.

Previously, Mulholland *et al.* [9] published an article outlining a compact device capable of generating all the required wavelengths for optically cooling and trapping Yb^+ ions. Within this article it is stated that ~100 µW of continuous wave (CW) emission are required for the cooling transition at 369.5 nm. It is further stated that this wavelength is generated by second harmonic generation using a 739 nm pump source, owing to the relative ease by which a 739 nm source may be frequency stabilised to an iodine reference. In light of these power and pump wavelength requirements, VECSELs offer an ideal route to generate emission of adequate power and spectral purity within a highly compact footprint while still maintaining close to diffraction limited spatial beam quality.

The first VECSEL to realise emission around 740 nm was published in 2009 by Schlosser *et al.* [10]. This benchmark-setting work highlighted a series of InP/AlGaInP quantum dot semiconductor disk laser gain structures which were capable of direct CW emission between 716 and 755 nm, and with powers up to 52 mW. Building on the progress of this work, we are able to demonstrate nearly triple the output power and that the laser can, at modest powers, emit on a single external cavity axial mode, making it ideally suited to second harmonic generation in PPLN waveguides. We acknowledge the recently published work of Nechay *et al.* [11], which, using the same gain sample wafer, reached approximately 350 mW of power, but with significantly broader emission spectrum, and at 741 nm.

In the context of Yb^+ ion cooling, the natural linewidth of the cooling transition is approximately 20 MHz, and hence it is important that any laser addressing this transition oscillates on a single axial mode when operating passively, so that this may be actively stabilised to reduce both the linewidth of the laser, if required, as well as the long term drift. Through careful microcavity design, class-A laser dynamics [12], high finesse external cavities, and an exceptionally low Schawlow–Townes linewidth limit, the supported noise bandwidth in a VECSEL can be very narrow even in free running operation. Accordingly, VECSELs may require only low modulation bandwidth active feedback on the external cavity length for wavelength stabilisation. This is in contrast to diode lasers, for example, which typically require high modulation bandwidth current servos in addition to mechanical feedback. Recently, a record low, sub-kHz linewidth emission from a VECSEL was demonstrated by Moriya *et al.* [13] using only piezoelectric modulation of the external cavity length.

Here we present a characterisation of a VECSEL gain structure where we achieve up to 22 mW of single axial mode operation at 740 nm using the combined effect of the SiC heat spreader etalon effect and a 2 mm thick quartz birefringent filter (BRF). Furthermore, we achieve spectral tunability down to 737.3 nm. Beyond 22 mW the laser exhibits multi-axial mode operation, and at best we achieve 150 mW of output power around 739 nm. The results in this work represent a proof of principle demonstration that optical powers are achievable with VECSELs at this wavelength, in line with future development of PPLN waveguides for generating 369.5 nm light.

1. Experimental configuration

The VECSEL gain structure active region consists of four groups of three $Al_{0.14}GaAs$ quantum wells (QWs). The QWs are 7 nm thick and, within each group, are separated from each other by 8 nm barrier layers of $Al_{0.4}GaAs$. The middle QW of each group is placed at a field antinode within the gain structure microcavity by using a 47 nm thick AlGaInP cladding layer, such that their geometric centers are 100 nm apart. Forming the distributed Bragg reflector are 33.5 pairs of AlAs/$Al_{0.28}GaAs$ layers, each of which are $\lambda/4$ thick, and both the gain microcavity and the Bragg reflector are designed around a wavelength of 750 nm. The specifics of the gain structure growth are described in further detail in reference [11]. The wafer is cleaved into chips approximately 4×4 mm in area and capillary bonded to 5×5 mm chips of silicon carbide (SiC) such that the SiC is an intra-cavity element. We yielded two successfully bonded samples (which were adjacent at the time of cleaving) that shall be referred to as samples 1 and 2. The bonded samples are clamped individually into a copper heat sink mounts with a 100 μm thick layer of indium foil between the copper and the SiC as a thermal compound. Temperature control of the gain medium is achieved via PID servo controlling a thermoelectric element which sinks heat into a secondary, water cooled, copper block. The gain sample temperature is maintained at around 4°C in order to blue shift the gain spectrum. We use dry nitrogen to prohibit water condensation on the gain chip.

The external cavity, shown schematically in Fig. 1, is formed between a plane output coupler (OC) mirror and the gain structure DBR, with a 100 mm radius of curvature high reflector (HR) mirror in between acting as a fold mirror. The gain sample to the curved fold mirror

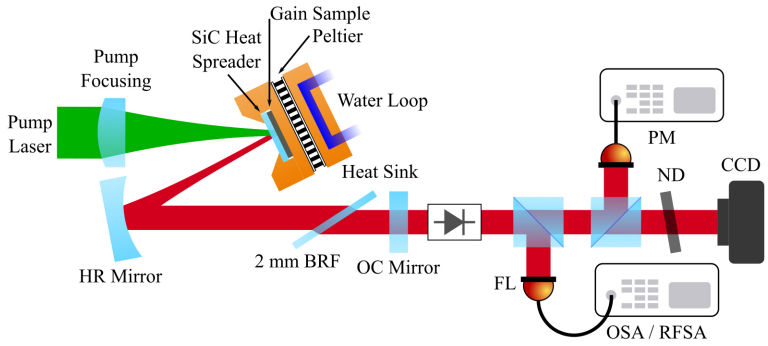

Fig. 1. Schematic of the VECSEL cavity design and surrounding experimental setup. The distances from the gain sample to the fold mirror, and fold mirror to output coupler mirror are 55 mm and 200 mm respectively, and the 2 mm thick birefringent filter is positioned in the cavity mode at Brewster's angle. A Faraday isolator is positioned after the OC mirror to reduce emission instability caused by spectral reflections. A portion of the beam is coupled to a fiber and is used to determine the optical spectrum and the RF spectrum. The remaining beam is then split again so that the beam power can be measured on a power meter, and the spatial profile can be captured on a CCD camera after suitable neutral density attenuation.

separation is approximately 55 mm, and the curved mirror to OC (R = 98 % @ 740 nm) separation is approximately 200 mm. In this configuration, the laser cavity fundamental spatial mode has a radius of ~48 µm ($1/e^2$) at the gain surface. The external cavity fold full angle is ~24°, and the mode radii at the plane OC mirror are, respectively, 244 µm and 295 µm in the tangential and sagittal directions.

A Spectra Physics Millennia EV laser emitting at 532 nm is used to pump the VECSEL. The pump light is brought to a waist with a 75 mm focal length achromatic doublet which is mounted to a linear translation stage. As this lens creates a waist smaller than the external cavity laser spatial mode at the gain sample position (waist), the pump focusing lens is defocused so as to match the pump spot size with the laser mode size. In order to tune the spectral emission, and to aid in reducing the emission bandwidth, the 2 mm thick BRF is incorporated into the external cavity. The filter is placed at Brewster's angle, and rotated around the axis orthogonal to the plane of the filter optical surface to achieve the desired emission wavelength. On account of the SiC heat spreader acting as an etalon, spectral tuning is achieved in increments of approximately 0.3 nm, and is shown in Fig. 2. Upon emission from the external cavity, a Faraday optical isolator is used to attenuate back reflections from subsequent optics. Following the isolator, the beam is split into three beams for spectral and optical power analysis, as depicted in Fig. 1.

2. VECSEL Characterisation

The primary objective is to demonstrate that both samples could generate sufficient optical power at 739 nm for second harmonic frequency generation of 369.5 nm light. At a heat sink temperature of 20°C, the peak performance of the gain structure occurs at approximately 755 nm. Once the temperatures of samples 1 and 2 were set to 4°C and 3°C respectively, rotating the BRF angle enabled tuning of the optical spectrum; as demonstrated in Fig. 2. Regarding the relatively coarse spectral tuning steps, it is noted that a slightly wedged heat spreader - such as the diamond employed in [11] - could significantly reduce the etalon effect on the wavelength tuning of the laser, however this may incur the cost of increased emission linewidth. From the experiment, the shortest achievable emission wavelengths were 738.25 nm for sample 1 and 737.3 nm for sample

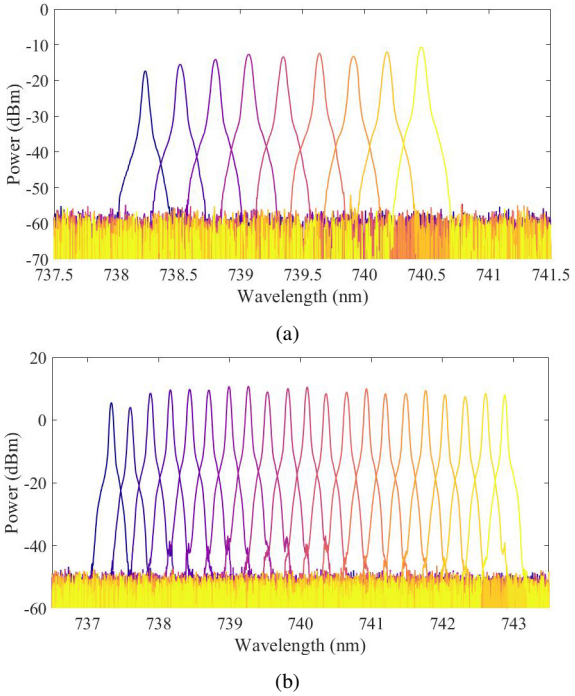

Fig. 2. Optical tuning performance of the two gain samples around 739 nm via rotation of the intra-cavity BRF. Figures (a) and (b) correspond to samples 1 and 2 respectively.

2; see Figs. 2a and 2b. Beyond these wavelengths, further tuning of the BRF would result in either the laser switching off, or the emission jumping to the opposite end of the gain spectrum provided that the adjacent BRF transmission maximum fits within this bandwidth. In the case of low pump powers, it was typical for the laser to cut out, whereas for higher pump powers, the emission spectrum would typically jump to the longer wavelength BRF transmission peak at approximately 770 nm. For sample 1, the -3dB spectral width is approximately 0.04 nm for all pump powers, and this value corresponds to the resolution limit of the OSA to within a factor of two. For all pump powers used with sample 1, the emission spectrum was contained within a single SiC etalon free spectral range. The same behavior was not replicated with sample 2 however, whereby the laser would start to populate adjacent SiC etalon fringes with sufficient pump power. The data in Fig. 2b shows the spectrum under the condition that the pump power has been reduced so that that laser only emits within a single SiC etalon fringe. We expect that the incorporation of an additional BRF (of thickness ≥ 4 mm) into the external cavity would limit the spectral width to a single SiC etalon fringe.

With the 2 mm BRF optimised in each case for emission at 740 nm, data for the emitted power as a function of the absorbed pump power was recorded, and is given in Fig. 3. For this data, we make the approximation that the absorbed pump power is given by the difference between the pump power incident on the sample and the total power that is reflected from the gain sample. For sample 1 with an output coupling of 2 %, we calculate the slope efficiency to be 9.2 % using all data points in the region of 1.52 W and 2.68 W, and a threshold pump power of 1.52 W. Equally for sample 2 with the same output coupling percentage, we calculate the slope efficiency to be 8.3 %, with a threshold pump power of 1.27 W. Though sample 1 did not operate with an output coupling percentage of 4 % at 740 nm, we were able to operate sample 2 with this output coupler. The threshold power noticeably increases to 1.91 W, while the efficiency of the laser

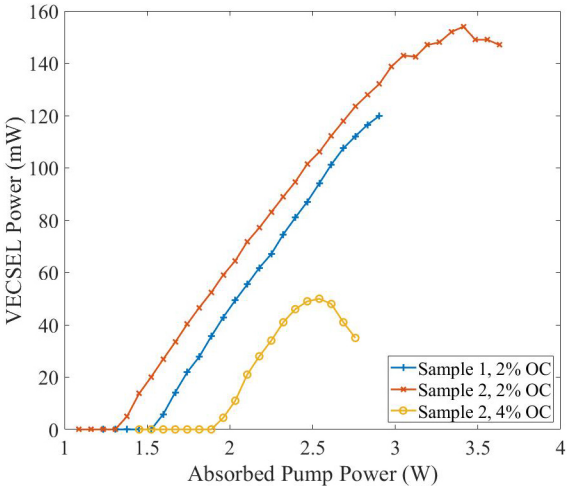

Fig. 3. VECSEL emission power as a function of absorbed pump power at 532 nm. Samples 1 and 2 are operating respectively at 740.1 and 740.6 nm.

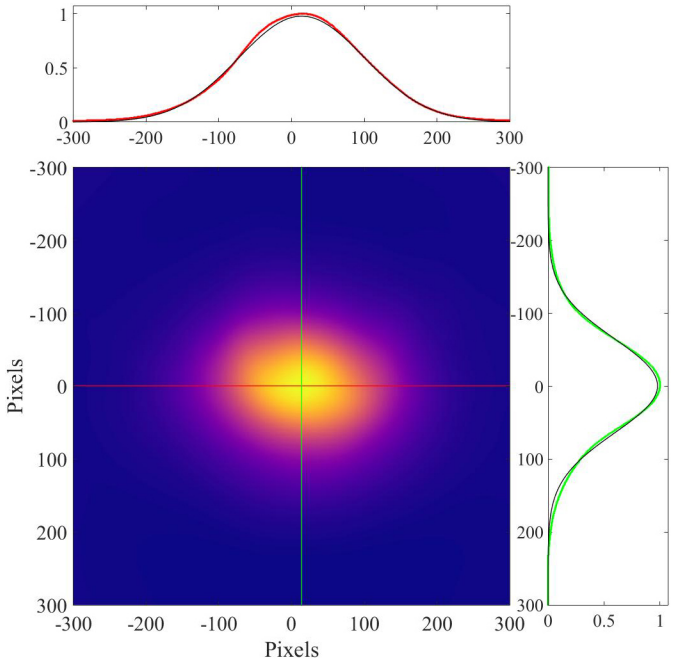

Fig. 4. Beam profile in the far field, approximately 100 cm from the OC mirror. The image has been smoothed in software to remove artefacts in the image caused by fringing effects in the neutral density filter in place between the laser and the imaging CCD, and dust on the optics.

also increases to approximately 10.2 %. At the peak before thermal rollover begins to dominate, sample 2 exhibits a maximum output power of 154 mW for 2 % of output coupling, and 50 mW for 4 % of output coupling. It is reasonable to conclude, therefore, that either sample 2 exhibits marginally more gain than sample 1 - which points to the significance of even the smallest spatial variations in the wafer growth - or, more likely, that the quality of the contact bond between the

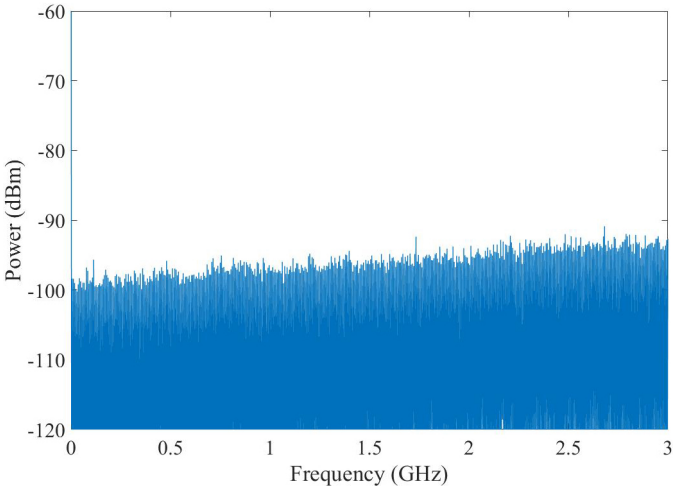

Fig. 5. Figure showing the RF spectrum of the VECSEL emission at a pump power of 1.74 W (~22 mW emission) for a spectral window of 3 GHz. The lack of significant beat frequencies at the external cavity FSR is indicative that the laser is operating on a single cavity axial mode. As the pump power was increased, the RF spectrum would show peaks intermittently up to approximately the fifth external cavity FSR frequency. VBW = RBW = 13 kHz.

gain and SiC heat spreader is reduced at the time of operating the laser, and by changing the output coupler mirror, the precise lasing spot on the sample is altered. All of these effects may curtail the maximum output power and thermal rollover of the laser with all other experimental parameters unchanged.

We note that sample 1 operated at a slightly shorter wavelength at the time of taking these data, and demonstrated a slightly narrower tuning range towards shorter wavelengths. Accordingly, it is a known consequence that by introducing increased losses to the laser - in this case by attempting to use the 4 % output coupler - the wavelength is blue shifted. As we are operating on the edge of the gain profile, it is likely that the wavelength is shifted to the point where the laser will not reach threshold.

Regarding the specific behaviour of sample 2 in combination with the 4% output coupler, we did not observe any change in the emitted polarisation state throughout the range of pump powers used, which is at odds with the behaviour reported in reference [11]. There are a number of experimental differences however which could explain such behaviour. Specifically, our spatial mode never deviated from a fundamental Gaussian, and we employ a thicker BRF, a smaller pump spot and mode radii, a lower heatsink temperature and a different pump area to fundamental mode area ratio. Further, we made no attempt to maintain the gain structure crystal plane [011] angle with respect to the bench or the axis around which the external cavity folds.

In Fig. 4 we show the spatial profile of the beam in the far field for sample 1, approximately 1 meter from the plane OC mirror. The image is captured using a 8-bit monochrome CCD camera. In order to capture the beam profile within the dynamic range of the sensor, a suitable combination of neutral density filters were used, which were positioned in the beam at an angle so as to avoid back reflections. In doing so, significant fringing effects were observed on the beam, which were subsequently filtered out of the image in processing in the inverse spatial domain. The line plots in Fig. 4 show the line data corresponding to the red and green lines also plotted in the figure, and the black curve in each case is a Gaussian least squares fit to the respective axes. Given the quality of the fit to the line data, we conclude that the beam from the

VECSEL is composed of only the fundamental spatial mode.

Throughout the experiments the laser operation was free running and no attempt to actively or passively stabilise the emission wavelength was made. The resolution limit of the OSA is 0.02 nm, which corresponds to approximately 10.9 GHz; this is well above the VECSEL external cavity free spectral range of 588 MHz. Fig. 5 shows the measured RF spectrum for sample 1 as the beam is incident onto a fiber coupled fast photodiode. The detector has a -3 dB bandwidth of 25 GHz, and approximately 10 % of the maximum permissible CW power was used for the measurement. The RF spectrum analyser resolution (RBW) and video (VBW) bandwidths were both set to 13 kHz. The lack of signal peaks at multiples of the external cavity FSR frequency indicates that the VECSEL is operating on a single axial mode of the external cavity. VECSELs are class A lasers, which implies that instabilities that give rise to a transient axial mode population often happen over a timescale that is slow in comparison to the inverse bandwidth of our photodetector and RFSA. As such, even constantly evolving axial modes in the laser cavity should coexist for sufficient time to be detected [14, 15]. In contrast to recent work [11], where a -3 dB linewidth of approximately 3 nm at 741 nm was reported, our laser cavity uses a 2 mm thick BRF instead of a 0.5 mm thick filter, and further we use a SiC heat spreader in place of diamond. The surface parallelism of SiC is significantly higher than for diamond, and hence offers a stronger etalon effect. The combined effect of this and the higher curvature around the peak transmission of the BRF is likely to be sufficient in promoting a significantly narrower emission spectrum.

3. Conclusions

We have demonstrated a VECSEL with native emission around 739 nm which operates on a single axial mode with up to 22 mW output power, and on multiple axial modes with up to 150 mW. For use in ion cooling and trapping, in order to achieve the desired 100 µW of optical power in the UV [9], a total conversion efficiency of only ~0.07% would be required from the VECSEL emission of 150 mW. In reference [8] we have superseded this efficiency figure whereby 1 mW of SHG signal was generated from 390 mW of VECSEL power, yielding a basic conversion efficiency of 0.26 %. Furthermore, the demonstrated beam profile of the laser at 739 nm shows excellent overlap with a fundamental Gaussian profile and hence lends itself well to future waveguide coupling. We anticipate that, in future, this laser will be a useful tool in combination with large-mode PPLN waveguides as a complete source of 369.5 nm light, as well as possible intra-cavity SHG experiments owing to the highly re-configurable nature of a VECSEL's external cavity. We have shown that single mode operation is achievable at 739.5 nm and we anticipate that to achieve higher power single axial mode operation throughout the output power range, a bespoke resonant periodic gain structure design should be realized with a single QW on E-field maxima, thereby providing further spectral filtering from the semiconductor micro-cavity, in conjunction with a BRF or group of BRFs [16], and the heat spreader etalon effect.

All data supporting this study are openly available from the University of Southampton repository at: https://doi.org/10.5258/SOTON/D1669

Funding

Egineering and Physical Sciences Research Council: (EP/T001046/1), Academy of Finland: (315121).

Acknowledgement

The authors would like to thank Patrik Rajala and Sanna Ranta for growth of the VECSEL structure, as well as EPSRC and the Academy of Finland for Funding.

Disclosures

The authors declare no conflicts of interest.

References

1. F. S. Cataliotti, E. A. Cornell, C. Fort, M. Inguscio, F. Marin, M. Prevedelli, L. Ricci, and G. M. Tino, "Magneto-optical trapping of Fermionic potassium atoms," Phys. Rev. A **57**, 1136–1138 (1998).
2. W. Süptitz, G. Wokurka, F. Strauch, P. Kohns, and W. Ertmer, "Simultaneous cooling and trapping of ^{85}Rb and ^{87}Rb in a magneto-optical trap," Opt. Lett. **19**, 1571–1573 (1994).
3. J. E. Simsarian, A. Ghosh, G. Gwinner, L. A. Orozco, G. D. Sprouse, and P. A. Voytas, "Magneto-Optic Trapping of ^{210}Fr," Phys. Rev. Lett. **76**, 3522–3525 (1996).
4. G. Uhlenberg, J. Dirscherl, and H. Walther, "Magneto-optical trapping of silver atoms," Phys. Rev. A **62**, 063404 (2000).
5. C. Roos, T. Zeiger, H. Rohde, H. C. Nägerl, J. Eschner, D. Leibfried, F. Schmidt-Kaler, and R. Blatt, "Quantum State Engineering on an Optical Transition and Decoherence in a Paul Trap," Phys. Rev. Lett. **83**, 4713–4716 (1999).
6. Z. Peng-Yi, X. Zhuan-Xian, L. Jie, H. Ling-Xiang, and L. Bao-Long, "Magneto-Optical Trapping of Ytterbium Atoms with a 398.9 nm Laser," Chin. Phys. Lett. **25**, 3631–3634 (2008).
7. R. Blatt, H. Schnatz, and G. Werth, "Ultrahigh-Resolution Microwave Spectroscopy on Trapped $^{171}Yb^{+}$ Ions," Phys. Rev. Lett. **48**, 1601–1603 (1982).
8. A. C. Gray, J. R. C. Woods, L. G. Carpenter, H. Kahle, S. A. Berry, A. C. Tropper, M. Guina, V. Apostolopoulos, P. G. R. Smith, and C. B. E. Gawith, "Zinc-indiffused MgO:PPLN waveguides for blue / UV generation via VECSEL pumping," Appl. Opt. **59**, 4921–4926 (2020).
9. S. Mulholland, H. A. Klein, G. P. Barwood, S. Donnellan, P. B. R. Nisbet-Jones, G. Huang, G. Walsh, P. E. G. Baird, and P. Gill, "Compact laser system for a laser-cooled ytterbium ion microwave frequency standard," Rev. Sci. Instruments **90**, 033105 (2019).
10. P. J. Schlosser, J. E. Hastie, S. Calvez, A. B. Krysa, and M. D. Dawson, "InP/AlGaInP quantum dot semiconductor disk lasers for CW TEM_{00} emission at 716 - 755 nm," Opt. Express **17**, 21782–21787 (2009).
11. K. Nechay, H. Kahle, J.-P. Penttinen, P. Rajala, A. Tukiainen, S. Ranta, and M. Guina, "AlGaAs/AlGaInP VECSELs with direct emission at 740 - 770 nm," IEEE Photonics Technol. Lett. **31**, 1245–1248 (2019).
12. G. Baili, M. Alouini, T. Malherbe, D. Dolfi, I. Sagnes, and F. Bretenaker, "Direct observation of the class-B to class-A transition in the dynamical behavior of a semiconductor laser," EPL (Europhysics Lett.) **87**, 44005 (2009).
13. P. H. Moriya, Y. Singh, K. Bongs, and J. E. Hastie, "Sub-kHz-linewidth VECSELs for cold atom experiments," Opt. Express **28**, 15943–15953 (2020).
14. M. E. Barnes, Z. Mihoubi, K. G. Wilcox, A. H. Quarterman, I. Farrer, D. A. Ritchie, A. Garnache, S. Hoogland, V. Apostolopoulos, and A. C. Tropper, "Gain bandwidth characterization of surface-emitting quantum well laser gain structures for femtosecond operation," Opt. Express **18**, 21330–21341 (2010).
15. C. R. Head, K. G. Wilcox, A. P. Turnbull, O. J. Morris, E. A. Shaw, and A. C. Tropper, "Saturated gain spectrum of vecsels determined by transient measurement of lasing onset," Opt. Express **22**, 6919–6924 (2014).
16. A. L. Bloom, "Modes of a laser resonator containing tilted birefringent plates," J. Opt. Soc. Am. **64**, 447–452 (1974).